Desalination and Water Treatment
www.deswater.com
doi: 10.5004/dwt.2021.26658

214 (2021) 181–193
February

Polyester membranes as 3D scaffolds for cell culture

Monika Wasyłeczko[a,*], Wioleta Sikorska[a], Małgorzata Przytulska[a], Judyta Dulnik[b], Andrzej Chwojnowski[a]

[a]*Department of Biomaterials and Biotechnological Systems, Nałęcz Institute of Biocybernetics and Biomedical Engineering, Polish Academy of Sciences, Trojdena 4 str., 02-109 Warsaw, Poland, emails: mwasyleczko@ibib.waw.pl (M. Wasyłeczko), wsikorska@ibib.waw.pl (W. Sikorska), mprzytulska@ibib.waw.pl (M. Przytulska), achwojnowski@ibib.waw.pl (A. Chwojnowski)*
[b]*Laboratory of Polymers and Biomaterials, Institute of Fundamental Technological Research, Polish Academy of Sciences, Pawińskiego 5B str., 02-106 Warsaw, Poland, email: jdulnik@ippt.pan.pl*

Received 9 April 2020; Accepted 25 May 2020

ABSTRACT

The study presents two types of three-dimensional membranes made of the biodegradable copolymer. They were obtained by the wet-phase inversion method using different solvent and pore precursors. In one case, a nonwoven made of gelatin and polyvinylpyrrolidone (PVP) as precursors of macropores and small pores, respectively, were used. In the second case, PVP nonwovens and Pluronic were used properly for macro- and micro-pores. As the material, a biodegradable poly(L-lactide-co-ε-caprolactone) is composed of 30% ε-caprolactone and 70% poly(L-lactic acid) was used. Depending on the pore precursors, different membrane structures were obtained. The morphology of pores was studied using the MeMoExplorer™, an advanced software designed for computer analysis of the scanning electron microscopy images. The scaffolds were degraded in phosphate-buffered saline and Hank's balanced salt solutions at 37°C. Moreover, the porosity of the membranes before and after hydrolysis was calculated.

Keywords: 3D scaffolds; Poly(L-lactide-co-ε-caprolactone); Porosity of membrane; Phase inversion method; Degradation of scaffolds

1. Introduction

Semipermeable membranes are used in various areas of technology like chemical (including petrochemical), food and drink industry, water purification, pharmaceutical, and biomedical application including tissue engineering [1–10]. Tissue engineering as a scientific discipline proposes new alternatives for the treatment by transplantation of biological material that would replace, maintain, or restore function to damaged tissues or whole organs [11,12]. Depending on the application, the membrane should have appropriate properties such as biocompatibility, morphology, mechanical properties, non-toxicity, and even bioresorbability. For the tissue regeneration process, it is necessary to obtain appropriate porous scaffolds as a support for cells during *in vitro* culture with various growth factors. The use of spatial structures determines the functioning of cells and facilitates obtaining the desired tissue [13–17].

One of the most important parameters of the scaffolds for cell culture is morphology and more precisely – porosity. The size and number of pores have a huge impact on cell penetration into the membrane, their migration, proliferation, production of extracellular matrix (ECM), as well as diffusion of nutrients, oxygen, and removal of metabolites outside the scaffold [14,18,19]. To obtain the adequate pore size, the pore precursors such as salts [20], polymers [21,22–24], and nonwovens [25,26] are used. The size of the pore is properly defined by the purpose of the research,

* Corresponding author.

among other for which kind of cells they will be intended [14,16,18]. For example, working with chondrocytes requires smaller pores than working with stem cells for chondrogenesis [25,27,28]. It will be different from hepatocytes [29] or with osteoblasts [28,30]. Moreover, to obtain adequate morphology of the membranes the various methods are used, such as 3D print, phase separation, gas foaming, particulate leaching, selective laser sintering, electrospinning, or freeze-drying [13,18,26,27,31,32].

Further important parameter during the production of scaffolds is material. It should be characterized by biocompatibility, appropriate strength properties (modulus of elasticity, compressive, and tensile strength, stiffness, etc.), biodegradability (the speed must be carefully selected for the formation of a new tissue structure), or bioresorbability. The degradation products should not be toxic to the body and need to be excreted from the body. The most commonly biomaterials used for scaffolds are natural and synthetic polymers, or their combination. Examples of natural materials for scaffolds are gelatine, chitosan, alginate, and hyaluronic acid. They are characterized by high biocompatibility and biodegradability but their drawback is among other solubility in an aquatic environment and not enough mechanical strength [15,19,33–35]. The most common synthetic materials are the aliphatic polyesters: polylactide (PLA), polycaprolactone (PCL), polyglycolide (PGA), or their copolymers like poly(L-lactide-co-ε-caprolactone) (PLCA). Polyesters are biocompatible polymers with good mechanical strength which degrade to non-toxic products that are easily removed from the organism [15,33,35–38].

The article presents the formation of biocompatible, semipermeable, three-dimensional scaffolds of degradable co-polyester PLCA. Depending on the micro-, macropores precursors used a different membranes morphology was obtained. Structure analysis was performed by using scanning electron microscopy (SEM). The porosity assessment was made by a computer program, the MeMoExplorer™ used to analyzing SEM images. The usage and description of the program have been presented in previous works [39–41]. Furthermore, the degradation assessment of the scaffolds was performed in simulated physiological conditions using phosphate-buffered saline (PBS) and Hank's balanced salt solution (HBSS) at 37°C. Weight loss, pH of media, and SEM of samples were used to monitor the degradations.

Such membranes can be used in tissue engineering, in which scientists are still looking for new scaffolds for cell culture.

2. Experimental

2.1. Materials

Copolymer of L-lactide and ε-caprolactone in a 70/30 molar ratio was purchased from Corbion. Polyvinylpyrrolidone (PVP) 10 kDa, phosphate buffer solution (PBS), Pluronic® F127, sodium bicarbonate, sodium azide (NaN_3), sodium chloride, potassium chloride, phenol red, monopotassium phosphate (KH_2PO_4), D-glucose, disodium phosphate, magnesium sulfate, and calcium chloride were purchased from Sigma-Aldrich. 1,4-Dioxane,chloroform were procured from POCh SA. Methanol and ethanol were purchased from Linegal Chemicals. The pork gelatin and PVP nonwovens (Fig. 1) were obtained by an electrospinning method in the Institute of Fundamental Technological Research PAS.

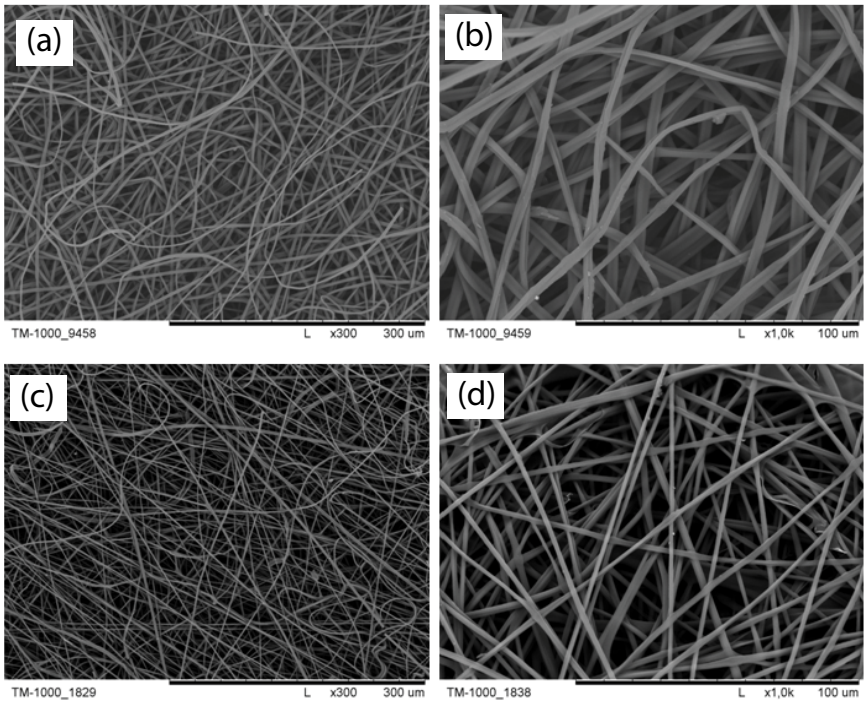

Fig. 1. Photomicrographs of pork gelatin (a and b) and PVP nonwovens (c and d) obtained by an electrospinning method. Magnification 300× (a and c) and 1,000× (b and d).

The deionized water (18.2 MΩ cm conductivity) was obtained using Mili-Q apparatus (Milipore).

2.2. Preparation of scaffold using PVP nonwoven (PLCA1)

The PLCA and pluronic polymers were dissolved in dioxane with constant stirring to obtain 10 wt.% concentration with 4:1 ratio of PLCA:Pluronic. A polymer mixture was poured onto the cooled glass base (4°C) and its thickness was set to 2 nm, after which the PVP layer was laid. Then another portion of polymers was poured to saturate the nonwoven, again a second slice of nonwoven and third layer of membrane forming solution were added. All layers were pressed and the air was removed using a Teflon roller. Received membrane was gelled in a bath with deionized water with ice (about 4°C). The prepared membranes were stored in 70% ethanol. It is important to protect the PVP nonwoven from water to prevent its dissolving.

2.3. Preparation of scaffold using gelatin nonwoven (PLCA2)

The PLCA and PVP polymers were dissolved in chloroform with constant stirring to obtain 10 wt.% concentration with 4:1 ratio of PLCA:PVP. The scaffold was made analogous to PLCA1 preparation. The only difference was that the gelation bath contained cooled methanol at 4°C and the obtained membrane was treated with warm water (50°C) to removed gelatin nonwoven. Similarly to PLCA1 scaffold, the prepared membranes were stored in 70% ethanol and the gelatin nonwoven need to be protected from water.

2.4. SEM observation

Morphology of top and bottom layers, and cross-section of scaffolds before and after hydrolysis were examined using a SEM (Hitachi TM – 1000) with an accelerator voltage of 15 kV. The samples were immersed into the ethanol for at least 15 min and then they were removed and put into liquid nitrogen in order to fracture them into pieces. Afterwards, the samples were dried and coated with a 7 nm layer of gold using a sputter coater (EMITECH K550X).

2.5. Estimate of pores in scaffolds by computer analysis of SEM images

For the analysis, the thirty SEM photomicrographs of cross-section and top layer of both scaffolds, before and after hydrolysis, were taken according to the description in section 2.4 (SEM observation). SEM images were taken with the same size (1,280 × 950 = 1,216,000 px = 182,681 μm^2, 100 μm = 258 pixels) with microscope magnification of ×300. Then they were analyzed by the MeMoExplorer software which involved selection and contouring of pores, measurement of their surfaces, partition of pores into various size, classes, and measurement of total areas (porosity coefficients) covered by pores of given classes. The received data can be processed statistically to obtaining parameters like average (Ave), standard deviation (SD), and instability coefficients (SD/Ave). That can be done by using a suitable software like Microsoft Excel.

2.6. Degradation of scaffolds at simulated physiological condition

The degradation of the scaffolds was performed in simulated physiological condition using PBS and HBSS. Both liquids were prepared in the laboratory. The PBS was prepared by dissolving the tablets in deionized water, while HBSS was prepared according to the method given in literature [42]. The scaffolds were cut into rectangles, which were measured (length, width, and thickness) using caliper and SEM tools and weighed by electronic balance (MATTLER TOLEDO KA-52c). The shape of membranes was different due to their specific structure and incapability to cut them out of a similar size. The weight of each sample was about 0.014 g. Samples of scaffolds (n = 6) were immersed into small, plastic cubs filled with 40 mL of PBS at pH 7.26 and HBSS at pH 7.78 (it was increased after the addition of sodium azide – bacteriostatic agent) for five (PLCA1) and four (PLCA2) weeks at 37°C. The time for PLCA2 has been shortened due to its rapid hydrolysis. Every week specimens were washed in deionized water, dried, weighed, and the pH-values of PBS and HBSS were monitored using an electrolyte-type pH meter (METTLER TOLEDO MP225). The mass loss was calculated from the following equation [43]:

$$\text{Weight loss} = \frac{\left(M_0 - M_t\right)}{M_0} \times 100\% \quad (1)$$

where M_0 and M_t with subscript 0 and t are masses at the immersion time of 0 and t, respectively. All the values presented were the average of six samples.

2.7. Porosity of scaffolds

The porosity of the scaffolds was determined by measuring the mass and dimensions of the scaffolds before and after hydrolysis, as described by Ho and Hutmacher [44]. It was calculated with the following formula:

$$\text{Porosity} = \frac{D_p - D_{\text{ap}}}{D_p} \times 100\% \quad (2)$$

where D_p is the density of PLCA (1.621 g/cm^3), D_{ap} is the apparent density (scaffold mass/apparent scaffold cube volume). The calculations were carried out in 10 repetitions for both scaffolds before hydrolysis and five repetitions after hydrolysis.

All data were expressed as average (Ave) ± standard deviation (SD).

3. Results and discussion

The main aim in preparation of scaffolds for cell culture is to use appropriate biocompatible material and obtain an adequate three-dimensional network of interconnected macropores. The top layer of scaffolds need to be perforated to enable cells to enter the membrane and the bottom surface should be dense to prevent them from leaving the membrane. Moreover, membrane (including the inner pore walls) need to be semipermeable which is obtained

by using micropores precursor like PVP or Pluronic. Small pores are necessary for migration of nutrients, oxygen, or metabolites.

3.1. Characterization of PLCA1 and PLCA2 scaffolds

Advantage of nonwovens used as non-classical pore precursors, is that they are located during preparation in the whole volume of the membrane-forming solution, which guarantees even distribution of macropores, throughout the scaffold. Depending on the pore precursors used, different size of pores were obtained.

The SEM micrographs of PLCA1 scaffold present an irregular structure with macropores, obtained using PVP nonwovens (Fig. 2). The perforation gaps of PLCA1 surface (Figs. 2a–c) are from 20 to 400 μm size. The interior (Figs. 2d–f) is a three-dimensional network of interconnected macropores from 20 to even 500 μm diameter.

The inner walls of membrane are porous and have uneven surface with protruding parts of the polymer that can facilitate cell adhesion. The addition of Pluronic affects microporous morphology. The bottom layer of PLCA1 is compact with nano-sized micropores (Figs. 2d–h). Likewise to the PLCA1, the SEM images of the PLCA2 scaffolds show a three-dimensional structure (Fig. 3).

The top layer contains many pores from 30 to 150 μm size (Figs. 3a–c). The cross-section creates a network of interconnected macropores between 50 and 350 μm length and from 20 to 250 μm width (Figs. 3d–f). They are smaller and definitely more numerous compared to the PLCA1 scaffold. Visible microporous structure (Figs. 3c, f, and h) is due to the addition of 10 kDa PVP. The bottom layer is dense with visible small pores up to 15 μm diameter (Figs. 3g–f). The average thickness of both scaffolds is about 700–1,200 μm and it depends on the thickness of the used nonwovens.

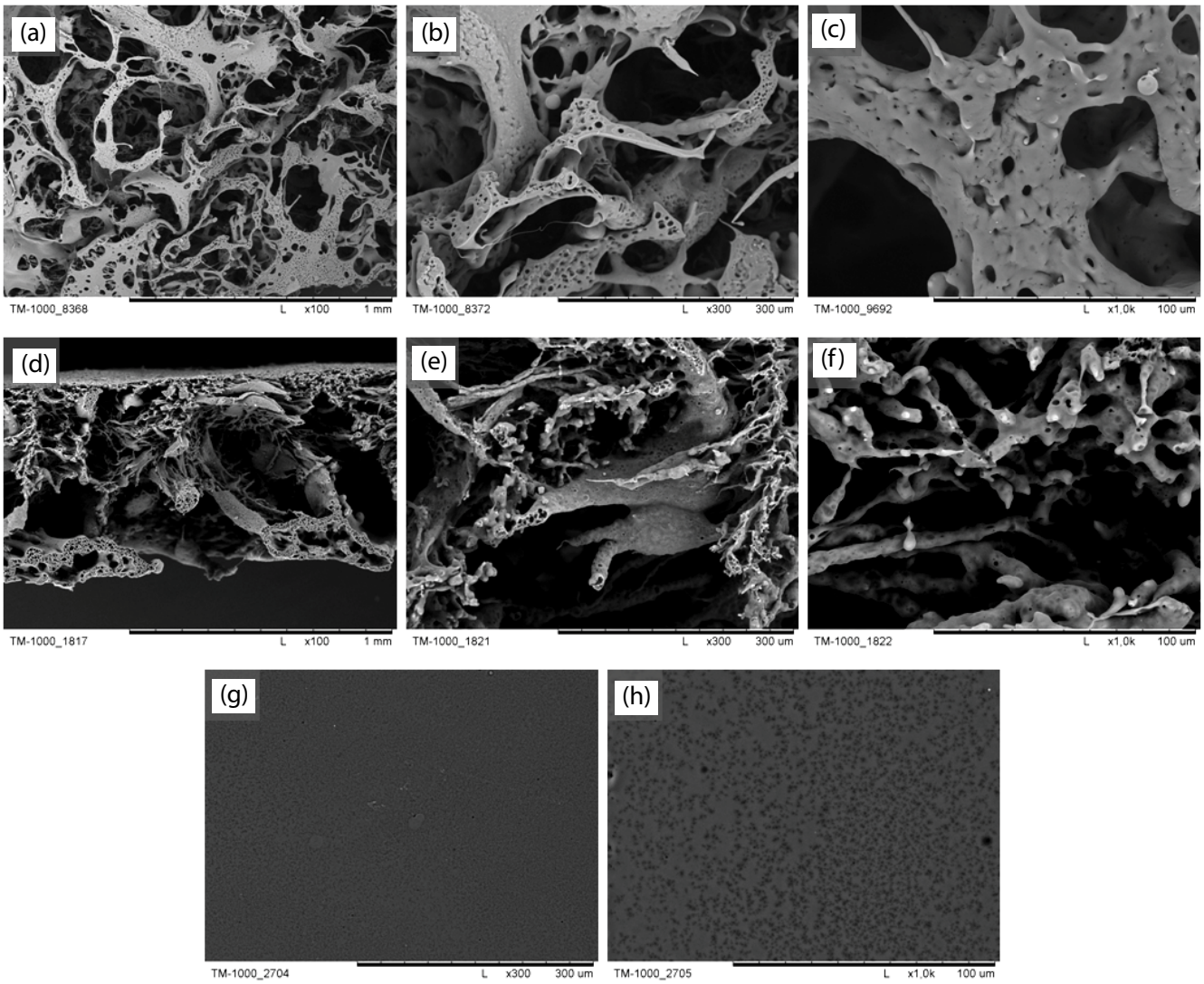

Fig. 2. SEM photomicrographs of the PLCA1 scaffold: (a–c) perforated skin layer; (d–f) cross-section; (g–h) dense bottom layer. Scale bars: (a and d) 1 mm; (b, e, and g) 300 μm; (c, f, and h) 100 μm.

Both scaffolds have a perforated skin layer that allows cells to enter them. The interior of both membranes has an irregular network of interconnected macropores that provides an appropriate environment for migration, proliferation, and adhesion of cells and is suitable for the production of ECM, protein. The selection of the nonwoven material as a pore precursor determines the shape of pores in the membrane. Through the choice of nonwovens, it is possible to control the size of the macropores, the thickness of the walls between pores, and width of scaffolds. Despite similar nonwovens structure of PVP and gelatin, the differences in membranes structures are significant. The larger pores with many protruding polymer parts are obtained using PVP nonwoven for PLCA1 membrane (Fig. 2). On the other hand, PCLA2 scaffold, where macropore precursor is gelatin nonwoven, has smaller, more numerous, and repeatable pores (Fig. 3). Microporous structure of both scaffolds results from using PVP 10 kDa and Pluronic to membrane-forming solution. Such construction ensures access to nutritious substances, oxygen, or allows for the removal of metabolic products from the interior of scaffolds. The bottom skin layer is compact that prevents cells and protein particles to get away out from scaffolds.

3.2. Hydrolysis of scaffolds at simulated physiological condition

To simulate physiological conditions, the PBS and HBSS fluids were used to determine the degradation rate of scaffolds. Especially, the Hank's balanced salt solution has a similar inorganic ion composition compared to blood plasma [45]. The samples for degradation were different in size due to the various construction of the scaffolds. For PLCA1 average size was 0.66 cm × 1.2 cm × 0.08 cm and for PLCA2 was 0.9 cm × 1.2 cm × 0.11 cm. The weight for PLCA1 was approximately 0.013 g and for PLCA20.015 g. The hydrolysis time for PLCA1 was 5 weeks but for PLCA2, it was only 4 weeks due to faster destruction of the PLCA2 sample at 37°C.

After hydrolysis in HBSS, in both scaffolds numerous cracks and enlargement of pores were visible (Figs. 4 and 5).

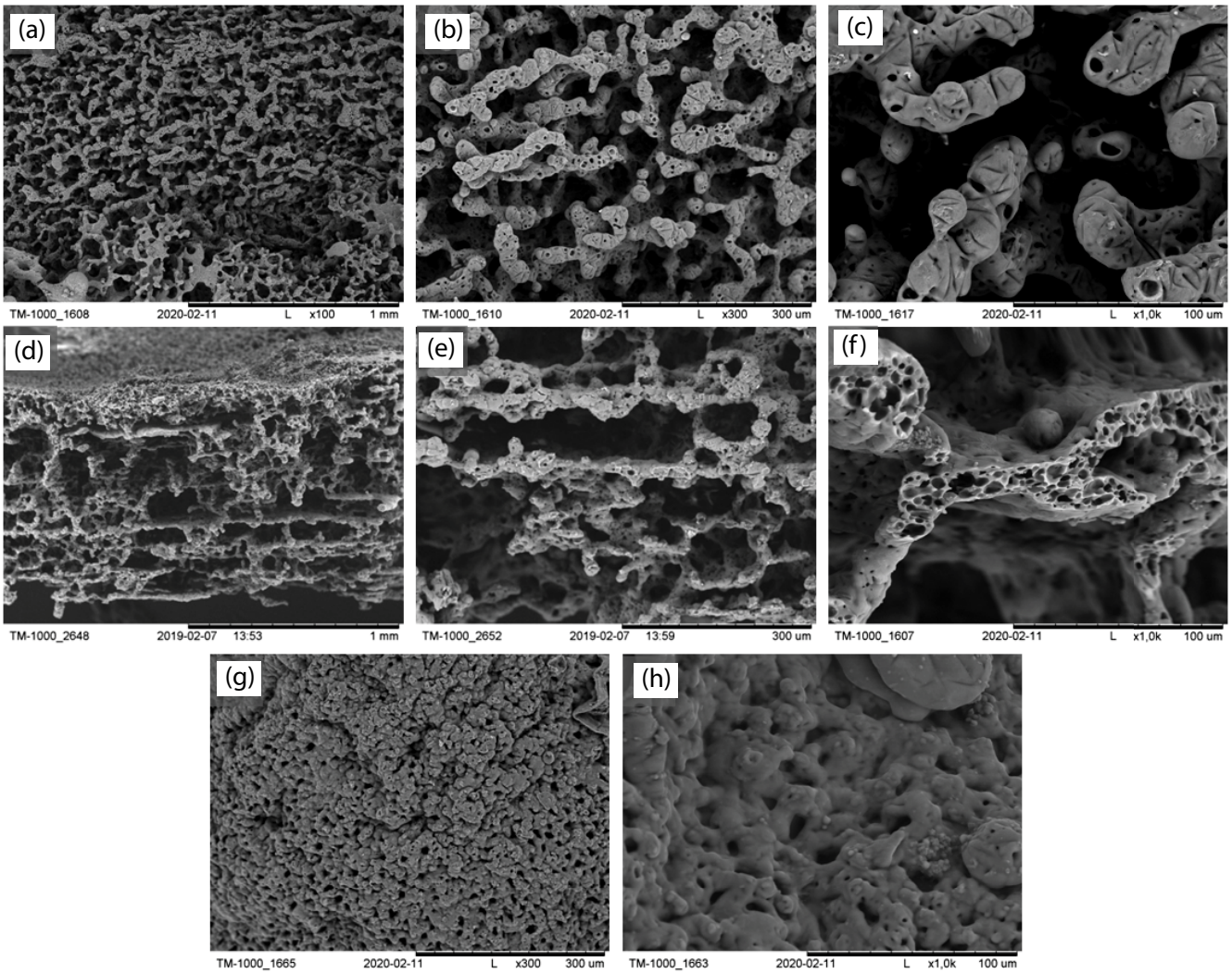

Fig. 3. SEM photomicrographs of the PLCA2 scaffold: (a–c) perforated skin layer; (d–f) cross-section; (g–h) dense bottom layer. Scale bars: (a and d) 1 mm; (b, e, and g) 300 μm; (c, f, and h) 100 μm.

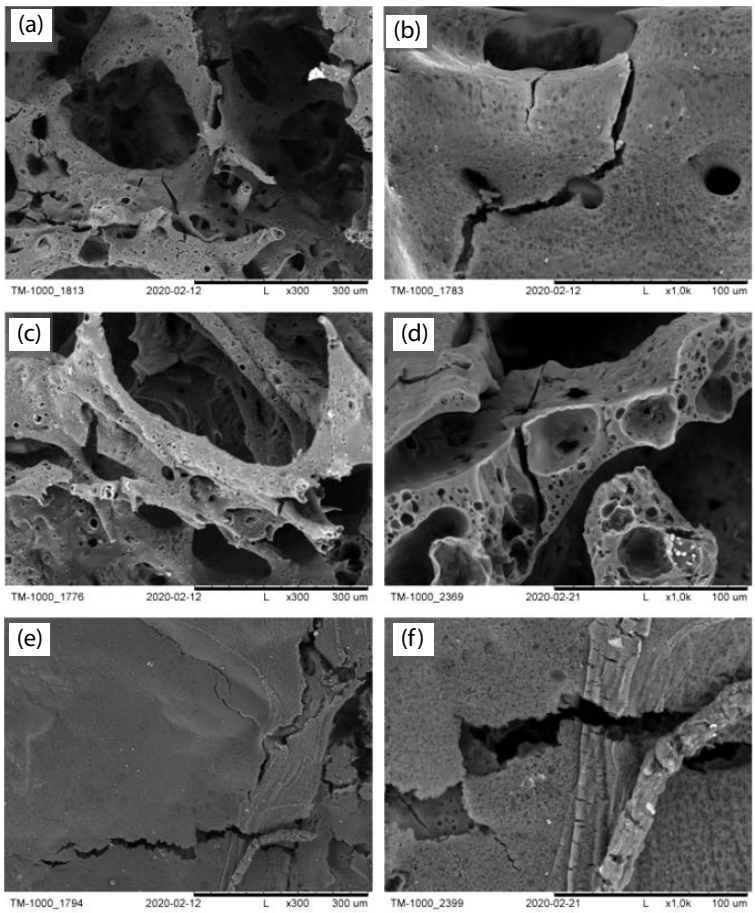

Fig. 4. SEM photomicrographs of the PLCA1 after hydrolysis in HBSS: (a and b) perforated skin layer; (c and d) cross-section; (e and f) dense bottom layer. Scale bars: (a, c, and e) 300 μm; (b, d, and f) 100 μm.

Similar breaks are noticeable on the SEM images in both scaffolds after hydrolysis in PBS (Figs. 6 and 7). However, more cracks can be observed after degradation in HBSS.

Fig. 8 shows the changes in pH medium during hydrolytic degradation in PBS and HBSS media. In both cases, there was a decrease of pH, which can be explained by the presence of the lactic and/or caproic acids formed as a result of polyester hydrolysis. The scaffolds' masses were evaluated before and after hydrolysis to check the impact of the PBS and HBSS medium on membranes (Figs. 9 and 10).

The percentage of weight loss in PBS up to the second week was initially slow, especially for PLCA1, only about 2% and 15% for PLCA2 and then significantly activated. On 28th day, an increase in weight loss can be seen for PLCA2 up to 49%, while for PLCA1 only to 12%, where it increases to 17% after 5 weeks. Definitely slower degradation is in the case of the PLCA1 scaffold. The weight loss of scaffolds in HBSS fluid is higher than was observed in the PBS medium, especially for PLCA2 (Fig. 10). After 4 weeks, the degradation rate of PLCA2 is about 71% and for PLCA1 five times less, about 14% and it increases to around 20% in 35 d. For both membranes, an increase in weight loss can be seen especially after 3 weeks.

The resume results of weights change before and after hydrolysis are shown in Table 1.

The weights are presented as an average of all samples before (n = 12) and after (n = 6) hydrolysis. The loss of weight is observed for both membranes in the range from 17 to 72 of the weight percentage. Due to the similar composition of HBSS to blood plasma [45], it can be stated that the degradation of the PLCA2 scaffold in the body can occur earlier than for PLCA1. It can also be seen that the decrease in pH is not rapid (Fig. 8), which should not have a negative effect on the body like the occurrence of inflammation.

3.3. Pore distributions for scaffolds before and after hydrolysis

The aim of MeMoExplorer™ is a precise measurement of pores present in the membranes for estimation of their size distribution and preparation of data for a statistical analysis that can be performed using software like the Microsoft Excel. The size of the pores was analyzed based on thirty SEM images for each cross-section and top layer of both scaffolds. In Table 2, the area of pores in eight size classes is presented. The results show the average percentage of appropriate pore size in relation to the whole SEM photomicrographs size.

In both scaffolds, the largest number of pores are those of an area over 300 μm^2. This is noticeable for cross-section and surface of both membranes. Above 1% or even about

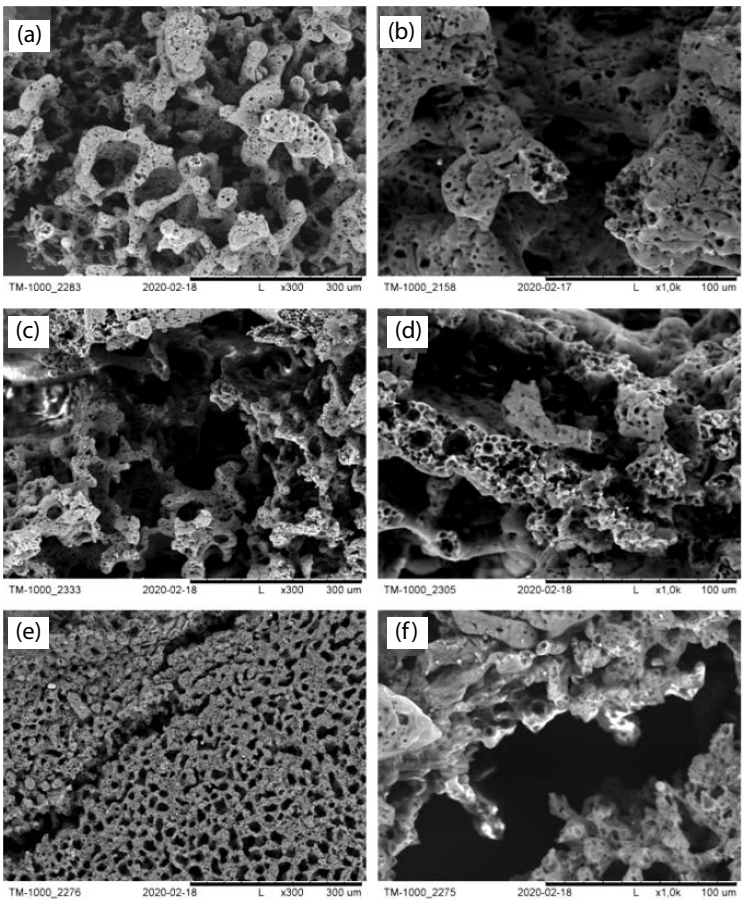

Fig. 5. SEM photomicrographs of the PLCA2 after hydrolysis in HBSS: (a and b) perforated skin layer; (c and d) cross-section; (e and f) dense bottom layer. Scale bars: (a, c, and e) 300 μm; (b, d, and f) 100 μm.

Table 1
Average weights of scaffolds before and after hydrolysis

Scaffold/medium	Weight before hydrolysis (g)	Weight after hydrolysis (g)	Weight loss after hydrolysis (%)
PLCA1/PBS	0.0129 ± 0.0030	0.0107 ± 0.0030	17
PLCA2/PBS	0.0143 ± 0.0023	0.0073 ± 0.0014	50
PLCA1/HBSS	0.0142 ± 0.0043	0.0113 ± 0.0043	20
PLCA2/HBSS	0.0128 ± 0.0030	0.0037 ± 0.0012	72

2% are the pores with 20–80 μm^2, while about 1% are the pores with 150–300 μm^2. Furthermore, the program provides data on the total number of pores (porosity coefficient). The porosity values for top-layers and cross-sections of scaffolds and also the difference between them are presented in Table 3. In addition, a comparison of pores after hydrolysis in PBS and HBSS was made.

The porosity coefficient in the cross-section before and after hydrolysis is higher for PLCA1 compared to PLCA2 membrane. The difference is not significant (0.42%). It is different for the top layer, where the areas of pores are higher even up to 1% for PLCA2. An increase in pore surface is noticeable in each case after hydrolysis, especially in HBSS medium. The most appreciable change is for the top layer of the PLCA2 where the increase is by almost 7%.

3.4. Coefficients of dissimilarity of pore size of scaffolds

Furthermore, computer analysis of the obtained SEM images is intended to evaluate the reproducibility of obtaining parameters in scaffolds production process (instability coefficient). It is calculated by the ratio of standard deviation (SD) of the porosity coefficient to averaged value (Ave) of the porosity coefficient estimated in the set of SEM images. The pore repeatability was also studied after hydrolysis. In Fig. 11 coefficients of dissimilarity, before and

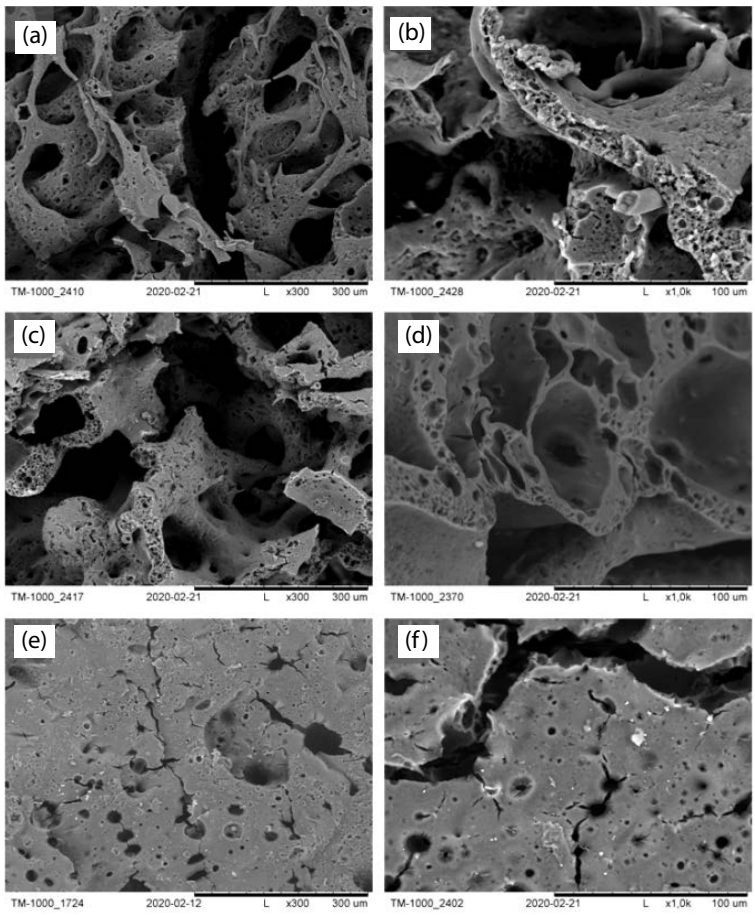

Fig. 6. SEM photomicrographs of the PLCA1 after hydrolysis in PBS: (a and b) perforated skin layer; (c and d) cross-section; (e and f) dense bottom layer. Scale bars: (a, c, and e) 300 μm; (b, d, and f) 100 μm.

after hydrolysis, of cross-section for both membranes are presented.

In Fig. 12, the instability coefficient, before and after degradation, for the top layer of both membranes is presented.

The cross-section and top layer of PLCA2 scaffold appeared to be the best one from the stability point of view. The instability coefficient is the smallest for this sample and it is only about 0.15. A stabilizing effect is observed in each case for both membranes, before and after hydrolysis, indicating the repeatability of the pore size. It is generally low and does not exceed 0.17 for cross-section and 0.30 for the top layer of both scaffolds.

3.5. Porosity of membrane

For biomedical applications pore size and porosity of scaffolds are critical factors to consider. Depending on the obtained parameters, it is possible to select appropriate cells for the experiment. In the study, the porosity of scaffolds was measured before and after hydrolysis (Fig. 13, Table 4). Results show that membranes obtained with addition of PVP nonwoven with pluronic (PLCA1) and gelatin nonwoven with PVP pore precursors (PLCA2) are characterized by a high porosity, about 95%. The higher value of this parameter was observed for membranes obtained with gelatin nonwoven and PVP 10 kDa added to polymeric solution. But this difference was not significant, just only about 2%. After degradation this value is increases, especially for PLCA2 in HBSS.

In Fig. 13, the abbreviation Diff means difference between porosity of PLCA1 or PLCA2 before and after degradation in PBS and HBSS media. The largest dissimilarity in porosity is observed in HBSS medium for PLCA2 and it is 2.61%, where as for PLCA1 it is 1.44%. In the case of degradation in PBS, the porosity difference is higher for PLCA2 again and equals 1.63%, while for PLCA1 it is only 0.38% that is more than four times less than for PLCA2 hydrolysis in PBS. In Table 4, the porosity values before and after degradation of the scaffolds are presented. In addition, the difference between the PLCA1 and PLCA2 are calculated.

The difference in the increase in porosity between PLCA2/HBSS and PLCA1/HBSS is over 3.1% as a result of its faster degradation.

Such scaffolds could be used for culture of microorganisms with the possibility of using in biotechnology. For example, as immobilization carrier to support the formation of biofilms in membrane reactors for water purification. Due to the presence of microbial cells, it is possible to significantly increase the efficiency of microbiological processes for removal or bioremediation of organic contaminants. In

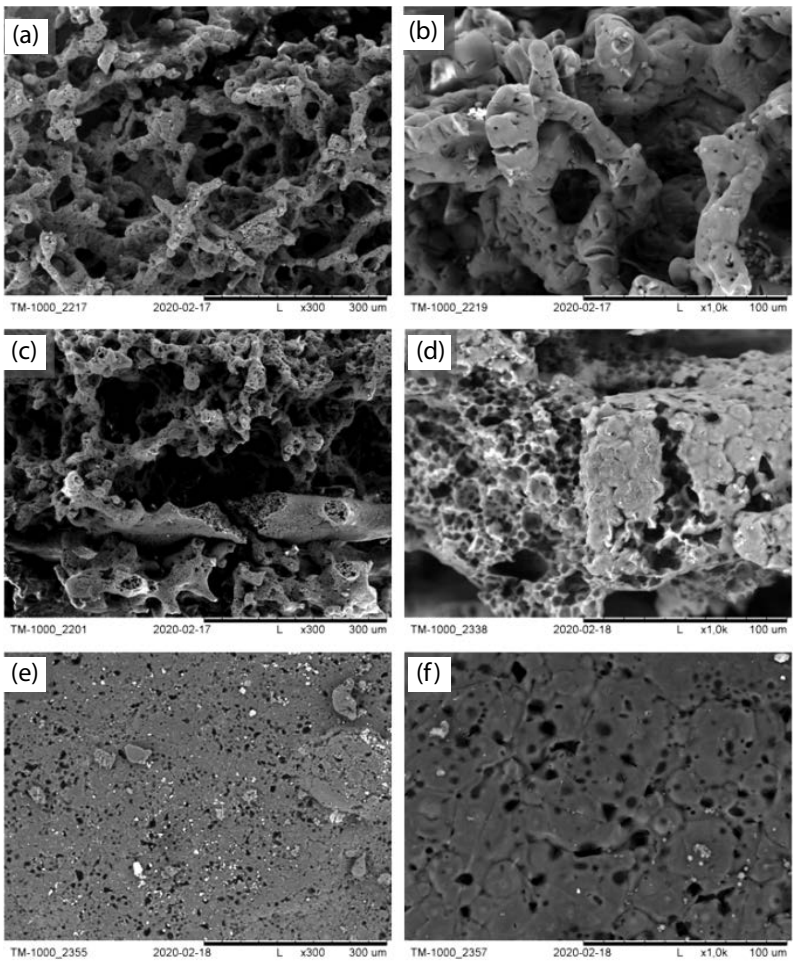

Fig. 7. SEM photomicrographs of the PLCA2 after hydrolysis in PBS: (a and b) perforated skin layer; (c and d) cross-section; (e and f) dense bottom layer. Scale bars: (a, c, and e) 300 μm; (b, d, and f) 100 μm.

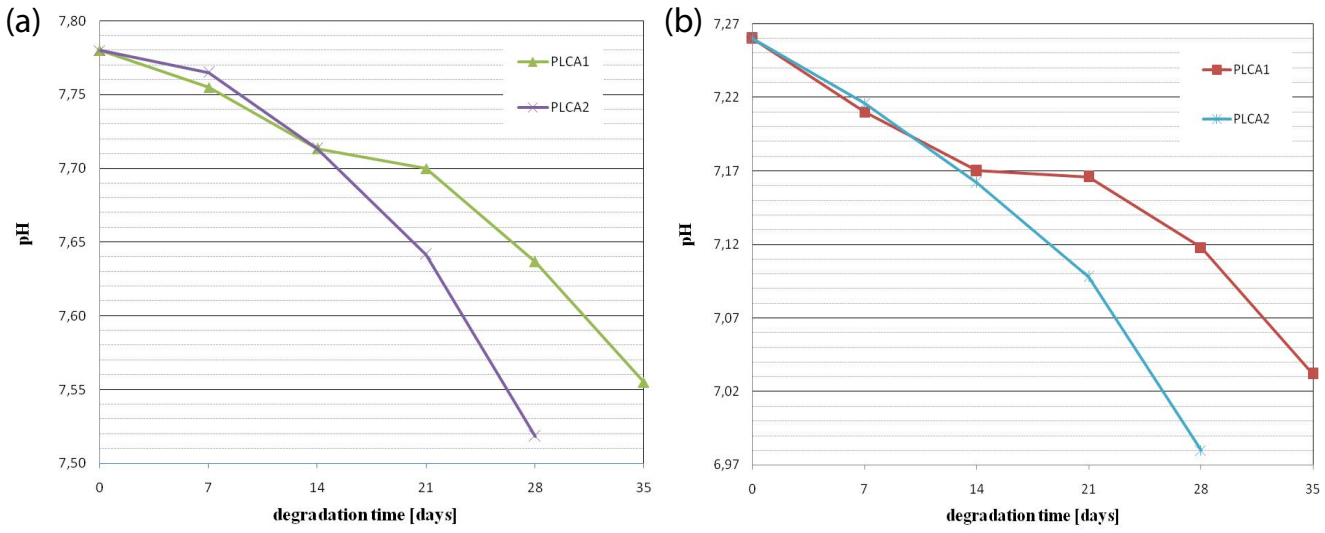

Fig. 8. Change in pH of HBSS (a) and PBS (b) medium during degradation of the PLCA1 and PLCA2 scaffolds.

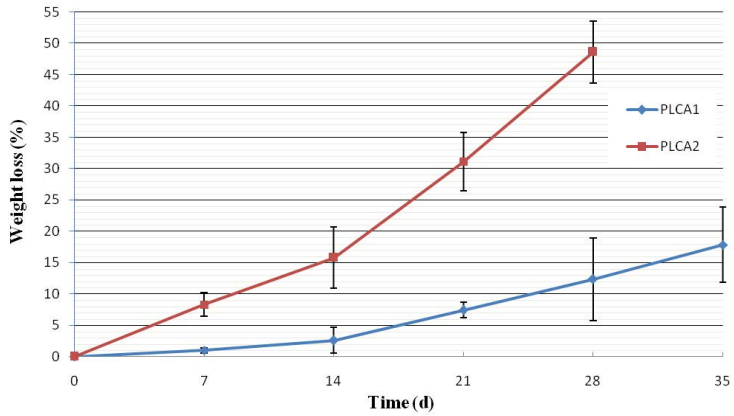

Fig. 9. Weight loss of PLCA1 and PLCA2 scaffolds as a function of degradation time in PBS medium.

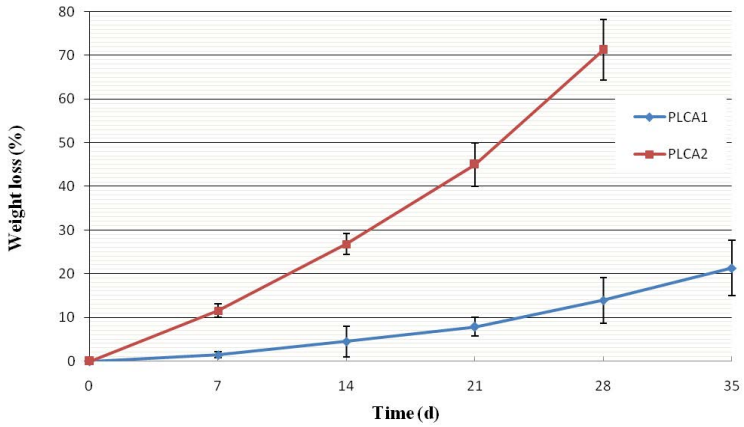

Fig. 10. Weight loss of PLCA1 and PLCA2 scaffolds as a function of degradation time in HBSS media.

Table 2
Average relative frequency of pores in eight size classes

Pore size (μm²)	0–3	3–8	8–20	20–80	50–100	100–150	150–300	>300
	(%)							
Cross-section of PCLA1	0.06 ± 0.02	0.20 ± 0.07	0.51 ± 0.21	1.63 ± 0.85	0.40 ± 0.25	0.73 ± 0.47	0.92 ± 0.53	42.73 ± 8.95
Cross-section of PCLA2	0.06 ± 0.03	0.18 ± 0.09	0.41 ± 0.23	1.14 ± 0.61	0.28 ± 0.17	0.54 ± 0.26	0.78 ± 0.40	43.37 ± 8.06
Top layer of PLCA1	0.07 ± 0.04	0.24 ± 0.11	0.55 ± 0.26	1.86 ± 0.96	0.55 ± 0.37	0.91 ± 0.50	1.19 ± 0.73	27.98 ± 8.43
Top layer of PLCA1	0.10 ± 0.03	0.34 ± 0.08	0.71 ± 0.15	1.51 ± 0.57	0.33 ± 0.29	0.71 ± 0.71	1.38 ± 1.02	29.26 ± 7.11

Table 3
Total areas of pores in relation to the whole SEM image size for cross-section and top layer of scaffolds

Scaffold/difference	Porosity coefficients before hydrolysis (%)	Porosity coefficients after hydrolysis in PBS (%)	Porosity coefficients after hydrolysis in HBSS (%)
Cross-section of PLCA1	47.18 ± 7.37	50.34 ± 8.08	51.32 ± 7.80
Cross-section of PLCA2	46.76 ± 7.04	47.38 ± 7.91	48.60 ± 7.40
Diff. between cross-section of scaffolds	0.42	2.95	2.72
Top layer of PLCA1	33.35 ± 7.05	36.41 ± 6.48	38.72 ± 6.67
Top layer of PLCA2	34.35 ± 5.36	40.15 ± 9.52	41.15 ± 11.56
Diff. between top layer of scaffolds	0.99	3.74	2.43

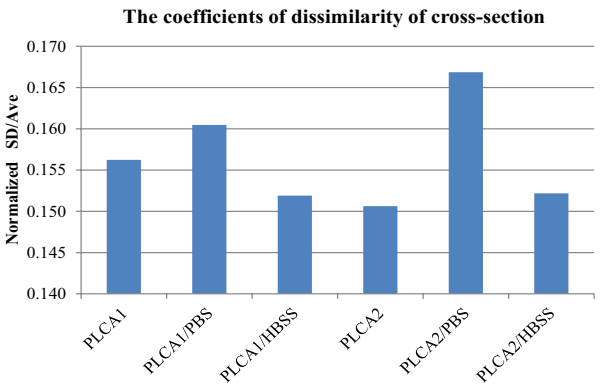

Fig. 11. Instability coefficients in cross-section of obtained scaffolds before and after hydrolyze.

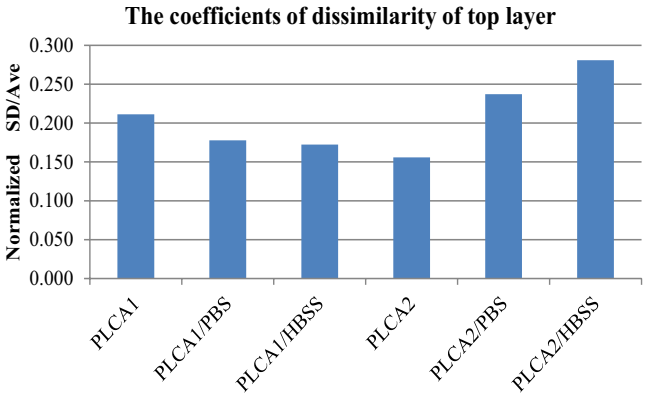

Fig. 12. Instability coefficients in the surface of obtained scaffolds before and after hydrolyze.

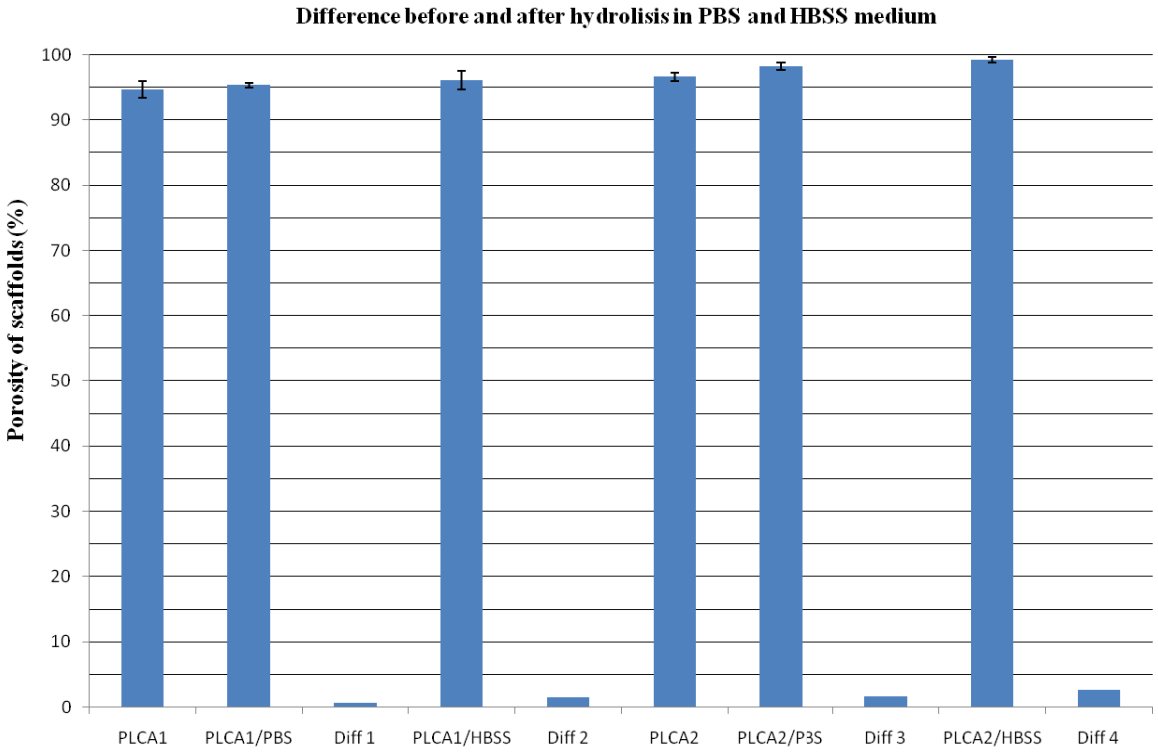

Fig. 13. Porosity of scaffold before degradation and difference between membranes of the same type after hydrolysis.

Table 4
Difference in porosity of scaffolds, before and after hydrolysis between PLCA1 and PLCA2

Scaffold/difference	Porosity before hydrolysis (%)	Porosity after hydrolysis in PBS (%)	Porosity after hydrolysis in HBSS (%)
PLCA1	94.67 ± 1.28	95.34 ± 0.38	96.11 ± 1.44
PLCA2	96.60 ± 0.68	98.23 ± 0.59	99.21 ± 0.44
Diff. between scaffolds	1.93	2.89	3.10

addition, microorganisms on a solid support are not leaching out of the bioreactor along with the flowing liquid. Porous membranes may also affect the selective delivery of substances, gases or removal of metabolites from the stream. Furthermore, polyester based biofilm carriers could be a carbon source to promote the growth of microorganisms [46–48].

4. Conclusion

The aim of this study was to obtain highly porous scaffolds for cell culture. Membranes were received by wet phase inversion using biocompatible PLCA material composed of 30% PCL and 70% PLA. The appropriate structure was achieved by the addition of selected macro- and micropore precursors. In both cases, the addition of PVP and gelatin nonwovens ensured a network of interconnected macropores, while Pluronic and PVP 10 kDa assured the microporous structure of both membranes. The scaffolds were hydrolyzed at simulated physiological conditions in PBS and HBSS, where weight loss, an increase of porosity, and a change in the structure and size of the pores were noted. The results are much more favorable after degradation in HBSS, especially in the case of PLCA2 in which gelatin nonwoven and PVP 10 kDa were used. Additionally, on the basis of computer analysis using the MeMoExplorer™ software, coefficients of dissimilarity of pore size were calculated. In each case is lower than 0.30, which indicates the repeatability in structure of scaffolds before and after degradation. However, the better and more promising results are for the PLCA2 scaffold, which can be used for further *in vitro* cellular studies.

References

[1] X. Zhenga, Z. Zhang, D. Yu, X. Chen, R. Cheng, S. Min, J. Wang, Q. Xiao, J. Wang, Overview of membrane technology applications for industrial wastewater treatment in China to increase water supply, Resour. Conserv. Recycl., 105 (2015) 1–10.

[2] A.K. Pabby, S.S.H. Rizvi, A.M.S. Requena, Membrane Separations - Chemical, Pharmaceutical, Food, and Biotechnological Applications, 2nd ed., CRC Press, New York, NY, 2015.

[3] N.L. Le, S.P. Nunes, Materials and membrane technologies for water and energy sustainability, Sustainable Mater. Technol., 7 (2016) 1–28.

[4] C. Xu, V.S. Thiruvadi, R. Whitmore, H. Liu, Delivery systems for biomedical applications: basic introduction, research frontiers and clinical translations, Biomater. Transl. Med., 5 (2019) 93–116.

[5] M. Takht Ravanchi, T. Kaghazchi, A. Kargari, Application of membrane separation processes in petrochemical industry: a review, Desalination, 235 (2009) 199–244.

[6] H. Lin, W. Gao, F. Meng, B.-Q. Liao, K.-T. Leung, L. Zhao, J. Chen, H. Hong, Membrane bioreactors for industrial wastewater treatment: a critical review, Crit. Rev. Environ. Sci. Technol., 42 (2012) 677–740.

[7] A. Ciechanowska, D. Schwanzer-Pfeiffer, E. Rossmanith, S. Sabalinska, C. Wojciechowski, J. Hartmann, K. Hellevuo, A. Chwojnowski, P. Foltynski, D. Falkenhagen, J.M. Wojcicki, Artificial vessel as a basis for disease related cell culture model, Int. J. Artif. Organs, 29 (2006) 1–4.

[8] M. Farina, J.F. Alexander, U. Thekkedath, M. Ferrari, A. Grattoni, Cell encapsulation: overcoming barriers in cell transplantation in diabetes and beyond, Adv. Drug Deliv. Rev., 139 (2019) 92–115.

[9] Y. Liu, J. Luo, X. Chen, W. Liu, T. Chen, Cell Membrane Coating Technology: A Promising Strategy for Biomedical Applications, Nano Microlett., 11 (2019) 1–46, doi: 10.1007/s40820-019-0330-9.

[10] G. Orive, D. Emerich, A. Khademhosseini, S. Matsumoto, R.M. Hernández, J.L. Pedraz, T. Desai, R. Calafiore, P. de Vos, Engineering a clinically translatable bioartificial pancreas to treat type I diabetes, Trends Biotechnol., 36 (2018) 445–456.

[11] K.M. Park, Y.M. Shin, K. Kim, H. Shin, Tissue Engineering and Regenerative Medicine 2017: A Year in Review, Tissue Eng. Part B, 24 (2018) 327–344.

[12] F. Berthiaume, T.J. Maguire, M.L. Yarmush, Tissue engineering and regenerative medicine: history, progress, and challenges, Annu. Rev. Chem. Biomol. Eng., 2 (2011) 403–430.

[13] A.A. Chaudhari, K. Vig, D.R. Baganizi, R. Sahu, S. Dixit, V. Dennis, S.R. Singh, S.R. Pillai, Future prospects for scaffolding methods and biomaterials in skin tissue engineering: a review, Int. J. Mol. Sci., 17 (2016) 1–31, doi: 10.3390/ijms17121974.

[14] I. Bružauskaitė, D. Bironaitė, E. Bagdonas, E. Bernotienė, Scaffolds and cells for tissue regeneration: different scaffold pore sizes—different cell effects, Cytotechnology, 68 (2016) 355–369.

[15] M.P. Nikolova, M.S. Chavali, Recent advances in biomaterials for 3D scaffolds: a review, Bioact. Mater., 4 (2019) 271–292.

[16] S.J. Hollister, Porous scaffold design for tissue engineering, Nat. Mater., 4 (2005) 518–524.

[17] F. Ahmadi, R. Giti, S. Mohammadi-Samani, F. Mohammadi, Biodegradable scaffolds for cartilage tissue engineering, Galen Med. J., 6 (2017) 70–80.

[18] Q.L. Loh, C. Choong, Three-dimensional scaffolds for tissue engineering applications: role of porosity and pore size, Tissue Eng. Part B, 19 (2013) 485–502.

[19] F.J. O'Brien, Biomaterials and scaffolds for tissue engineering, Mater. Today, 14 (2011) 88–95.

[20] X. Liang, Y. Qi, Z. Pan, Y. He, X. Liu, S. Cui, J. Ding, Design and preparation of quasi-spherical salt particles as water-soluble porogens to fabricate hydrophobic porous scaffolds for tissue engineering and tissue regeneration, Mater. Chem. Front., 2 (2018) 1539–1553.

[21] W. Zhao, Y. Su, C. Li, Q. Shi, X. Ning, Z. Jiang, Fabrication of antifouling polyethersulfone ultrafiltration membranes using Pluronic F127 as both surface modifier and pore-forming agent, J. Membr. Sci., 318 (2008) 405–412.

[22] B. Chakrabarty, A.K. Ghoshal, M.K. Purkait, Preparation, characterization and performance studies of polysulfone membranes using PVP as an additive, J. Membr. Sci., 315 (2008) 36–47.

[23] A.V. Bildyukevich, T.V. Plisko, A.S. Liubimova, V.V. Volkov, V.V. Ususky, Hydrophilization of polysulfone hollow fiber membranes via addition of polyvinylpyrrolidone to the bore fluid, J. Membr. Sci., 524 (2016) 537–549.

[24] G. Arthanareeswaran, D. Mohan, M. Raajenthiren, Preparation, characterization and performance studies of ultrafiltration membranes with polymeric additive, J. Membr. Sci., 350 (2010) 130–138.

[25] K. Dudziński, A. Chwojnowski, M. Gutowska, M. Płończak, J. Czubak, E. Łukowska, C. Wojciechowski, Three dimensional polyethersulphone scaffold for chondrocytes cultivation - the future supportive material for articular cartilage regeneration, Biocybern. Biomed. Eng., 30 (2010) 65–76.

[26] A. Chwojnowski, A. Kruk, C. Wojciechowski, E. Łukowska, J. Dulnik, P. Sajkiewicz, The dependence of the membrane structure on the non-woven forming the macropores in the 3D scaffolds preparation, Desal. Water Treat., 64 (2017) 324–331.

[27] G. Conoscenti, T. Schneider, K. Stölzel, F. Carfì Pavia, V. Brucato, C. Goegele, V. Carrubba, G. Schulze-Tanzil, PLLA scaffolds produced by thermally induced phase separation (TIPS) allow human chondrocyte growth and extracellular matrix formation dependent on pore size, Mater. Sci. Eng., C, 80 (2017) 449–459.

[28] M.J. Gupte, W.B. Swanson, J. Hu, X. Jin, H. Ma, Z. Zhang, Z. Liu, K. Feng, G. Feng, G. Xiao, N. Hatch, Y. Mishina, P.X. Ma, Pore size directs bone marrow stromal cell fate and tissue regeneration in nanofibrous macroporous scaffolds by mediating vascularization, Acta Biomater., 82 (2018) 1–11.

[29] P.L. Lewis, R.M. Green, R.N. Shah, 3D-printed gelatin scaffolds of differing pore geometry modulate hepatocyte function and gene expression, Acta Biomater., 69 (2018) 63–70.

[30] G. Turnbull, J. Clarke, F. Picard, P. Riches, L. Jia, F. Han, B. Li, W. Shu, 3D bioactive composite scaffolds for bone tissue engineering, Bioact. Mater., 3 (2018) 278–314.
[31] P. Denis, J. Dulnik, P. Sajkiewicz, Electrospinning and structure of bicomponent polycaprolactone/gelatin nanofibers obtained using alternative solvent system, Int. J. Polym. Mater. Polym. Biomater., 64 (2015) 354–364.
[32] R. Sakai, B. John, M. Okamoto, J.V. Seppälä, J. Vaithilingam, H. Hussein, R. Goodridge, Macromol. Mater. Eng. 1/2013, Macromol. Mater. Eng., 298 (2013) 45–52, doi: 10.1002/mame.201370001.
[33] R. Song, M. Murphy, C. Li, K. Ting, C. Soo, Z. Zheng, Current development of biodegradable polymeric materials for biomedical applications, Drug Des. Dev. Ther., 12 (2018) 3117–3145.
[34] L.S. Nair, C.T. Laurencin, Biodegradable polymers as biomaterials, Prog. Polym. Sci., 32 (2007) 762–798.
[35] F. Asghari, M. Samiei, K. Adibkia, A. Akbarzadeh, S. Davaran, Biodegradable and biocompatible polymers for tissue engineering application: a review, Artif. Cells Nanomed. Biotechnol., 45 (2017) 185–192.
[36] T. Urbánek, E. Jäger, A. Jäger, M. Hrubý, Selectively biodegradable polyesters: nature-inspired construction materials for future biomedical applications, Polymers, 11 (2019) 1–21, doi: 10.3390/polym11061061.
[37] D. Daranarong, P. Techaikool, W. Intatue, R. Daengngern, K. Thomson, R. Molley, N. Kungwan, L. Foster, D. Boonyawan, W. Punyodom, Effect of surface modification of poly(L-lactide-co-ε-caprolactone) membranes by low-pressure plasma on support cell biocompatibility, Surf. Coat. Technol., 306 (2016) 328–335.
[38] T. Li, L. Tian, S. Liao, X. Ding, S.A. Irvine, S. Ramakrishna, Fabrication, mechanical property and *in vitro* evaluation of poly(L-lactic acid-co-ε-caprolactone) core-shell nanofiber scaffold for tissue engineering, J. Mech. Behav. Biomed. Mater., 98 (2019) 48–57.
[39] W. Sikorska, C. Wojciechowski, M. Przytulska, G. Rokicki, M. Wasyłeczko, J.L. Kulikowski, A. Chwojnowski, Polysulfone–polyurethane (PSf-PUR) blend partly degradable hollow fiber membranes: preparation, characterization, and computer image analysis, Desal. Water Treat., 128 (2018) 383–391.
[40] M. Przytulska, J.L. Kulikowski, M. Wasyłeczko, A. Chwojnowski, D. Piętka, The evaluation of 3D morphological structure of porous membranes based on a computer-aided analysis of their 2D images, Desal. Water Treat., 128 (2018) 11–19.
[41] M. Przytulska, A. Kruk, J.L. Kulikowski, C. Wojciechowski, A. Gadomska-Gajadhur, A. Chwojnowski, Comparative assessment of polyvinylpyrrolidone type of membranes based on porosity analysis, Desal. Water Treat., 75 (2017) 18–25.
[42] W. Chrzanowski, E. Ali, A. Neel, D. Andrew, J. Campbell, Effect of surface treatment on the bioactivity of nickel – titanium, Acta Biomater., 4 (2008) 1969–1984.
[43] M. Ara, M. Watanabe, Y. Imai, Effect of blending calcium compounds on hydrolytic degradation of poly(DL-lactic acid-co-glycolic acid), Biomaterials, 23 (2002) 2479–2483.
[44] S.T. Ho, D.W. Hutmacher, A comparison of micro CT with other techniques used in the characterization of scaffolds, Biomaterials, 27 (2006) 1362–1376.
[45] J. Gonzalez, R.Q. Hou, E.P.S. Nidadavolu, R. Willumeit-Römer, F. Feyerabend, Magnesium degradation under physiological conditions – best practice, Bioact. Mater., 3 (2018) 174–185.
[46] Y. Zhao, D. Liu, W. Huang, Y. Yang, M. Ji, L.D. Nghiem, Q.T. Trinh, N.H. Tran, Insights into biofilm carriers for biological wastewater treatment processes: current state-of-the-art, challenges, and opportunities, Bioresour. Technol., 288 (2019) 1–14.
[47] Z.B. Bouabidi, M.H. El-Naas, Z. Zhang, Immobilization of microbial cells for the biotreatment of wastewater: a review, Environ. Chem. Lett., 17 (2019) 241–257.
[48] D. Lu, H. Bai, F. Kong, S.N. Liss, B. Liao, Recent advances in membrane aerated biofilm reactors, Crit. Rev. Environ. Sci. Technol., 50 (2020) 1–55, doi: 10.1080/10643389.2020.1734432.